Vibrational Neutron Spectroscopy of Collagen and Model Polypeptides

H. D. Middendorf,* R. L. Hayward,‡ S. F. Parker,§ J. Bradshaw,¶ and A. Miller‖

*Clarendon Laboratory, University of Oxford, Oxford OX1 3PU; ‡Department of Biochemistry, University of Edinburgh, Edinburgh EH8 9XD; §ISIS Facility, Rutherford Appleton Laboratory, Chilton, Didcot, OX11 0QX; ¶Department of Preclinical Veterinary Science, University of Edinburgh, Edinburgh EH9 1QH; ‖The Principal's Office, Stirling University, Stirling FK9 4LA, United Kingdom

ABSTRACT A pulsed source neutron spectrometer has been used to measure vibrational spectra (20–4000 cm^{-1}) of dry and hydrated type I collagen fibers, and of two model polypeptides, polyproline II and $(prolyl\text{-}prolyl\text{-}glycine)_{10}$, at temperatures of 30 and 120 K. The collagen spectra provide the first high resolution neutron views of the proton-dominated modes of a protein over a wide energy range from the low frequency phonon region to the rich spectrum of localized high frequency modes. Several bands show a level of fine structure approaching that of optical data. The principal features of the spectra are assigned. A difference spectrum is obtained for protein associated water, which displays an acoustic peak similar to pure ice and a librational band shifted to lower frequency by the influence of the protein. Hydrogen-weighted densities of states are extracted for collagen and the model polypeptides, and compared with published calculations. Proton mean-square displacements are calculated from Debye-Waller factors measured in parallel quasi-elastic neutron-scattering experiments. Combined with the collagen density of states function, these yield an effective mass of 14.5 a.m.u. for the low frequency harmonic oscillators, indicating that the extended atom approximation, which simplifies analyses of low frequency protein dynamics, is appropriate.

INTRODUCTION

Collagen is the principal protein constituent of a wide variety of connective tissues in animals. Its structure has been investigated extensively by electron microscopy and by diffraction techniques using x-rays and neutrons (Miller, 1984; Fraser et al., 1987; Wess et al., 1990). There are still many open questions related to the structure of less common types of collagen, to structural changes during assembly or in pathological conditions, and to the large-scale structure of biomolecular "composites" involving collagen. However, a clear consensus has emerged about the molecular structure, packing, and assembly of collagen I, the most common type (Fraser et al., 1987; Kadler, 1994).

The molecular dynamics of collagen is less well understood. Since the mid-1970s, a great deal of experimental and theoretical work has been devoted to the dynamics of globular proteins (Karplus and Petsko, 1990), motivated by the conviction that the large body of structural knowledge based on diffraction data needs to be extended into the time domain if we are to understand fully their functional properties. With fibrous proteins such as collagen, the emphasis is not so much on gaining a detailed picture of the dynamics of transient kinetic processes, but on interpreting mechanical properties (stress-strain curves, elastic moduli, rheological parameters) in terms of the underlying bonding patterns, force constants, and mobilities. DNA is the only fibrous biopolymer for which experimental work comparable in scope to that on globular proteins has been undertaken, and for which molecular interpretations of a wide range of dynamical phenomena are being developed. Similar data on collagen and other fibrous systems, by contrast, are still quite limited, and there have been few attempts to interpret them in the light of recent theoretical and computational advances in biomolecular dynamics.

During the 1980s, following the commissioning of powerful pulsed neutron sources and a new generation of spectrometers, the momentum-energy space accessible to inelastic neutron scattering (INS) techniques has expanded substantially. It has become possible to investigate the low frequency vibrational excitations of DNA (Grimm et al., 1987) and of proteins and model polypeptides with a resolution approaching that of routine infrared (IR) and Raman spectrometers (Middendorf, 1984; Middendorf and Randall, 1985; Martel, 1992), and to compare INS data with molecular dynamics calculations (Smith, 1991). In a pioneering study, Berney et al. (1987) examined the low frequency modes of collagen using one of the first pulsed neutron spectrometers (Chen et al., 1978). The well known complementary features of neutron spectroscopy (absence of selection rules, dependence on amplitude of atomic motions, hydrogen/deuterium contrast) can be fully exploited now (Middendorf, 1995). Taking advantage of these developments, we have embarked on a study of the neutron vibrational properties of collagen fibers (Bradshaw et al., 1992), and more recently of two model polypeptides, polyproline II (PPII) and $(prolyl\text{-}prolyl\text{-}glycine)_{10}$ $(PPG)_{10}$, at energy transfers between 20 and 4000 cm^{-1} and temperatures down to 30 K. In this paper we present and discuss results of this work.

Received for publication 9 September 1994 and in final form 24 April 1995.

Address reprint requests to Dr. H. D. Middendorf, Clarendon Laboratory, University of Oxford, Parks Road, Oxford OX1 3PU, UK. Tel.: 44-1442-863-828; Fax: 44-1865-272400; E-mail: hdm01@isise.rl.ac.uk.

0006-3495/95/08/660/14 $2.00

MOLECULAR PROPERTIES OF TYPE I COLLAGEN AND ITS MODEL POLYPEPTIDES

Type I collagen consists almost entirely of the characteristic triple-stranded helix seen in some portions of all collagens.

It occurs in tendon, skin, and bone, and has two identical α1(I) chains and one homologous but distinct α2(I) chain (Miller, 1984). The three polypeptide chains each have a repeating Gly-X-Y sequence where Gly is the amino acid glycine, and X and Y are any other amino acid, but are often the imino acids proline (almost exclusively X) and hydroxyproline (almost exclusively Y). X-ray diffraction of tendon collagen indicates a triple-helical arrangement of nearly equivalent scattering units. The diffraction pattern is dominated by a helix with pitch of ≈9.5 Å, ≈3.3 units/turn, and an axial rise per residue of 2.9 Å (Fraser et al., 1983). The triple-helical arrangement is favored by the presence of glycine at every third residue, reducing steric hindrance and providing an interchain hydrogen bond. The conformation of the backbone of each strand of the collagen molecule is close to that of the left-handed helices polyglycine II (PGII) (Crick and Rich, 1955) and PPII (Arnott and Dover, 1968), supercoiled in right-handed fashion and associated to form the triple helix. Synthetic polypeptides with the sequence $(PPG)_n$ also adopt the left-handed PPII type helix, and, furthermore, associate in a right-handed supercoiled triple-helical arrangement (Yonath and Traub, 1969; Okuyama et al., 1981). The helical parameters of the triple helix are similar to those of collagen. PGII, PPII, and $(PPG)_n$ thus represent model systems with close structural similarities to collagen.

In vivo, collagen molecules are packed in quasihexagonal fashion in bundles termed fibrils (Miller, 1984). The fibrils of tendon have the simplest organization of all collagenous connective tissue. The function of tendon is to transmit the contractile force of muscle to bone. Hence, it needs to be flexible but virtually inextensible. For this purpose, collagen fibrils are laid down in the tendon along the direction of the force. This simple structural organization and the negligibly low amounts of non-collagenous material (other than water) in tendons make them an ideal and frequently exploited source of collagen for structural investigations.

Three populations of bound water have been identified in tendon by nuclear magnetic resonance (NMR) (Peto et al., 1990), dielectric, and sorption experiments (Grigera and Berendsen, 1979). The most tightly bound fraction consists of two water molecules for every three amino acid residues, and provides water bridges between the three strands of the collagen molecule, linking backbone carbonyl groups (Ramachandran and Chandrasekharan, 1968). This represents a water content of 12.5% by weight (12.5 g water/100 g dry collagen). These water molecules behave anisotropically in NMR experiments (Peto et al., 1990). At 25% hydration, these sites are occupied ≈90% (Grigera and Berendsen, 1979). A second, less tightly bound fraction is localized in the interstices of the quasihexagonal packing arrangement. At least a further 35 g water/100 g dry collagen can be absorbed exclusively in this site, in the form of hydrogen-bonded chains of water molecules (Hoeve and Tata, 1978). These two fractions account for essentially all of the ≈25 g water/100 g dry collagen in our hydrated collagen samples. A third population of more loosely bound water can be absorbed in the ground substance in which the collagen fibrils are embedded. The ground substance also contains mucopolysaccharides totaling ≈2 g /100 g dry collagen.

MATERIALS AND METHODS

Neutron spectrometer and scattering kinematics

We have used TFXA, the time-focused crystal analyzer spectrometer at the ISIS Pulsed Neutron Facility (Rutherford Appleton Laboratory, Chilton, UK) (Penfold and Tomkinson, 1986; Windsor, 1981), to measure neutron spectra from dry and hydrated collagen fibers, and dry powders of PPII and $(PPG)_{10}$, the latter in either the hydrogenous form or with the amide hydrogen exchanged for deuterium. Spectra were recorded at 30 and 120 K for dry collagen, 35 K for hydrated collagen, and 30 K for the synthetic polypeptides. IR spectra were also obtained for both isotopomers of $(PPG)_{10}$ at room temperature and at 77 K.

Neutrons are scattered by atomic nuclei with interaction potentials that are spherically symmetric and of extremely short range ($\approx 10^{-4}$ Å). Compared with optical techniques, the essential differences are, first, that the scattering depends sensitively on isotopic composition, and second, that each elementary scattering event (i.e., neutron-nucleus collision) involves both energy transfer $\hbar\omega$ and momentum transfer $\hbar\mathbf{Q}$ (Berney and Yip, 1980; Windsor, 1981; Lovesey, 1984). The appropriate conservation equations are

$$\hbar\mathbf{Q} = \hbar(\mathbf{k}_o - \mathbf{k}_f) \qquad \text{(momentum)} \qquad (1)$$

and

$$\hbar\omega = E_o - E_f = \frac{1}{2}m(v_o^2 - v_f^2) = \frac{1}{2}(\hbar^2/m)(k_o^2 - k_f^2)$$

$$\text{(energy)} \qquad (2)$$

where $k=|\mathbf{k}|$, λ, v, and E denote the wavenumber, wavevector, wavelength, velocity and energy of incident neutrons (subscript o), or neutrons scattered into solid angle element $d\Omega$ around a scattering angle 2θ (subscript f). The neutron rest mass is m; $\hbar$ is Planck's constant divided by 2π. Modern instruments on pulsed neutron sources often work in "inverse" scattering geometry; the incident beam is not monochromatized before scattering (as on reactor sources), but consists of a train of intense, short pulses with a nearly "white" energy distribution up to the eV region (Windsor, 1981). During the dead times between pulses, energy analysis is performed on the scattered fraction of neutrons by a combination of time-of-flight, crystal reflection (pyrolytic graphite), and crystal filtering techniques (beryllium). The intensity histogram recorded by the detectors represents an energy-loss spectrum analogous to Stokes scattering in Raman spectroscopy. For the scattering geometry of TFXA, the effective scattering angle 2θ for all pencils of radiation backscattered from the sample (compare Fig. 1) is 135° so that $\cos 2\theta = \mathbf{k}_f \cdot \mathbf{k}_o / k_f k_o = -1/\sqrt{2}$. Solving Eqs.1 and 2 for Q^2 gives

$$Q^2 = k_f^2\,[2 + \varpi + (1 + \varpi)^{1/2}\sqrt{2}]\,; \quad \varpi = \hbar\omega/E_f \qquad (3a)$$

where $E_f = 31.86\ \text{cm}^{-1}$ is the "final" or analyzer energy. Here and throughout the following, we use optical wavenumbers as convenient energy units ($1\ \text{cm}^{-1} = 123.98\ \mu\text{eV}$). The significance of Q is that motions are probed over scale lengths $d = 2\pi/Q$, which go down from 2.2 to 0.4 Å as $\hbar\omega$ increases from 15 to 4000 cm^{-1}. The TFXA spectrometer is unique in that it allows both the low frequency region (with its intrinsically collective excitations) and the whole of the intermediate and higher $\hbar\omega$ region (nondispersive optical phonons, localized excitations) to be covered. The energy resolution of TFXA (Penfold and Tomkinson, 1986) can be expressed as

$$\delta E/E = 16.7(\hbar\omega)^{-3/2} + 0.0006(\hbar\omega)^{1/2} \qquad (3b)$$

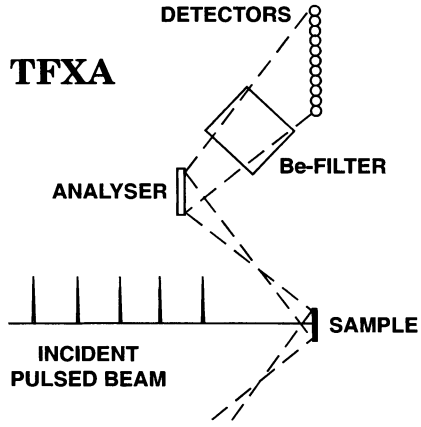

FIGURE 1 Scattering geometry of the spectrometer TFXA at ISIS. Only one limb of the symmetrical instrument configuration is shown.

It is ≈3% in the acoustic phonon region, decreasing to 1.4% between 200 and 300 cm^{-1}, and from there increasing again to values between 3 and 4% in the 3000–4000 cm^{-1} region.

In INS from biological macromolecules, the spectra measured are in general due to both incoherent and coherent scattering. The coherent component of the scattering is more informative in principle, but its energy-dependent properties (phonon bands, quasi-elastic broadening) are more difficult to isolate and to interpret (Jones, 1985; Bellissent-Funel et al., 1989). To illustrate the basic relations for the simple case of a monatomic assembly of target nuclei, the double differential cross section measured by a neutron spectrometer is given by

$$d^2\sigma/d\Omega dE = N(k/\hbar k_0) \times [b_{inc}^2 S_{inc}(Q, \omega) + b_{coh}^2 S_{coh}(Q, \omega)] \quad (4)$$

where N stands for the number of target nuclei, and b_{inc} and b_{coh} are incoherent and coherent scattering lengths, respectively. The dynamic structure factors $S_{inc}(Q, \omega)$ and $S_{coh}(Q, \omega)$, or "scattering laws," represent energy-resolved generalizations of the static structure factors $S_{inc}(Q) = 1$ and $S_{coh}(Q) \equiv S(Q)$ measured in diffraction experiments (Berney and Yip, 1980; Lovesey, 1984). The scattering of cold or thermal neutrons from any natural (i.e., not covalently deuterated) biopolymer is predominantly incoherent because of the large proton cross section of 80 barns versus an average of 5–6 barns for the heavier nuclei (1 barn = 10^{-24} cm^2).

Sample properties and preparation

Samples of Type I collagen used in these experiments were from the tail tendons of adult laboratory rats; the protein content is close to 98% of the dry weight. Synthetic PPII of mean molecular weight 6000 was purchased from Sigma Chemicals (Poole, UK); $(PPG)_{10}$ was purchased from Peptide Institute (Osaka, Japan).

We used fully hydrogenous samples of $(PPG)_{10}$, as well as deuterated samples, in which the labile amide hydrogens were exchanged for deuterium by soaking in 1% (v/v) acetic acid in D_2O for one week, exchanging the buffer, and soaking for a further week. We expected >95% exchange of amide hydrogen for deuterium in these samples. IR spectra confirmed this exchange (see Table 1), and indicated that the terminal carboxy group in each chain was protonated in the solid samples. In the following, when the context requires this, we will refer to the deuterated sample as $(PPG)_{10}$-d and to the hydrogenous one as $(PPG)_{10}$-h.

Dried samples of synthetic polypeptides were prepared by drying in vacuo for 72 h. $(PPG)_{10}$-h and $(PPG)_{10}$-d, dried in vacuo, contain approximately one water molecule per PPG triplet, equivalent to 6 g water/100 g completely dried $(PPG)_{10}$ (Sakakibara et al., 1972). This most tightly bound water molecule forms a hydrogen-bonded bridge between glycine and the second proline in the triplet. Recently x-ray diffraction of single crystals of the collagen model polypeptide $(ProHypGly)_4$-ProHypAla$(ProHypGly)_5$ (Bella et al., 1994) has directly demonstrated an interhelical network of hydrogen-bonded water between the closely packed cylindrical triple helices. In the $(PPG)_{10}$-d samples this water was exchanged for D_2O. Powder x-ray diffraction confirmed the expected triple-helical structure for both isotopomers and indicated hexagonal close packing of the cylindrical triple-helical molecules, each with a radius of ≈12.5 Å, in agreement with structural studies of PPG_{10} (Yonath and Traub, 1969). PPII dried in vacuo contains essentially no water. IR spectra of the polyproline sample con-

TABLE 1 Observed infrared spectra (FTIR) of $(PPG)_{10}$-h and $(PPG)_{10}$-d at 293 K, with amide band assignments

$(PPG)_{10}$-h	$(PPG)_{10}$-d	$(PPG)_{10}$-h from BBR		Assignments and comments
400 750		–		Very broad band carrying a few weak but distinct peaks, similar for $(PPG)_{10}$-h and $(PPG)_{10}$-d (≈60% intensity).
860 w	862 (65%)			
909 w	914 (40%)			
996 sh	996 (90%)			
1022 w	–			
	1031 w			
1042 w	1042 sh			
1089 w	1093 (50%)			
1158 w	1157 (70%)			
1205 m	1208 (70%)	1202		Proline
1242 m	1242 (50%)	1239	}	Amide III
1262 w	1269 (75%)	1263		
1331 m	1329 (100%)	1331		
1399 m	1400 (80%)	1400		
1447 s	1452 (100%)	1441		CH_2
1550 m	1550 (35%)	1543		Amide II
1637 vs	1637 (110%)	1642	}	Amide I
1662 sh	1662 (100%)	1666		
1775 w	– (nil)			

Frequencies in cm^{-1}. BBR = Brodsky-Doyle et al., 1975, Fig. 3 *a* and Table III. Percent values give approximate intensity changes relative to $(PPG)_{10}$-h (vs = very strong, s = strong, m = medium, w = weak, sh = shoulder).

firmed its type II left-handed helical structure (not shown). PPII has no labile hydrogens.

The "dry" collagen samples were prepared by drying over P_2O_5 in dry atmosphere for 72 h. They have a residual water content of 6 g/100 g completely desiccated collagen, representing the most tightly bound fraction of water, and similar to the residual water present in $(PPG)_{10}$ after drying in vacuo. The dry samples were handled in dry nitrogen gas atmosphere. D_2O-exchanged samples dried in this way were examined on the D17 neutron diffractometer at the Institut Laue-Langevin in Grenoble, France, and showed good crystalline order (Fig. 2).

H_2O-hydrated collagen fibers were prepared by exposure of fibers, soaked in H_2O, to atmosphere in equilibrium with a saturated solution of sodium chromate salt, at room temperature for 70 h. This provides a hydration of 25 g of H_2O/100 g of completely desiccated collagen. Completely desiccated collagen was prepared, for reference, by further drying of our "dry" samples over P_2O_5 *in vacuo* at 120°C for 7 h. Heating to this temperature is known to result in the loss of tightly bound water (Renugopalakrishnan et al., 1989).

Each collagen sample consisted of three layers assembled from several hundred fibers, giving final protein weights between 1 and 2 g. These and the powder samples (1–2 g) of synthetic polypeptides were contained in aluminum foil sachets and mounted in thin window aluminum containers in slab geometry on the TFXA spectrometer. The sample depth was ≈1 mm along the incident beam direction. The essentially flat background scattering from the empty aluminum container and foil contributed <0.5% to the total scattering and was subtracted in the data analysis.

RESULTS AND DISCUSSION

Basic aspects and overall properties of neutron spectra

Analysis and interpretation of the collagen spectra reported in this paper are based on the well established theory of neutron scattering from polymers and molecular crystals (Lynch et al., 1968; Berney and Yip, 1980; Windsor, 1981; Lovesey, 1984). In this section we discuss the overall properties of the spectra observed in terms of two basic processes: scattering from phonons and from localized oscillators. The theoretical framework for this is summarized in the Appendix. Spectral details and assignments to particular modes will be examined in subsequent sections.

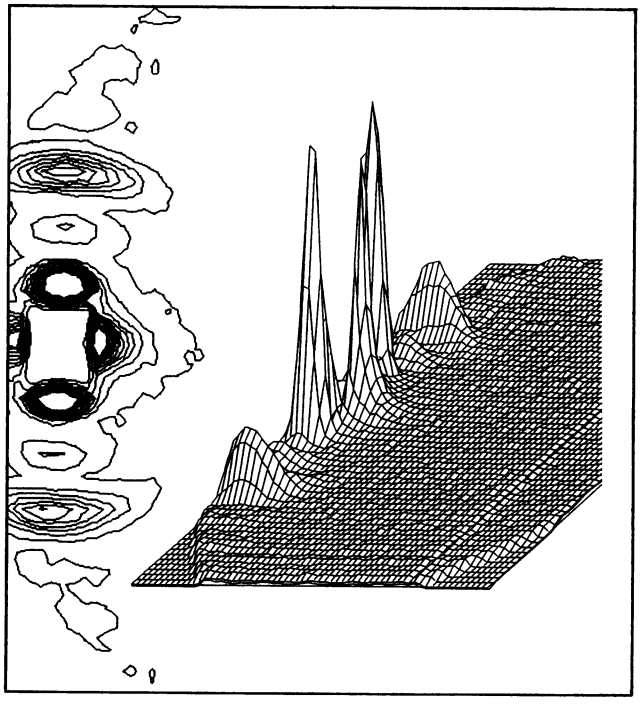

FIGURE 2 Neutron diffraction pattern from D_2O-exchanged collagen dried over P_2O_5, measured using diffractometer D17 at ILL Grenoble. Four to five meridional orders are seen (vertical sequence of maxima), the first at $Q = 0.0094$ A^{-1} corresponding to 670 Å.

Quantitatively, the distinction between low frequency phonon modes and localized group excitations at higher frequencies amounts to a time scale separation that is equivalent to a factorization of the incoherent intermediate scattering function (see Appendix). Such a factorization implies that the frequency of the localized oscillator should be large relative to the maximum frequency of the phonon band. Numerical calculations have demonstrated that this approximation remains useful even when this ratio is only of the order of 2 (Warner et al., 1983; Jobic and Lauter, 1988).

In practice we make a separation of our spectra at the band gap suggested by the intensity minimum between 360 and 400 cm^{-1}. In pursuing the resulting approximation, we are encouraged by the general results of normal mode analyses of peptide bond model molecules (Fillaux et al., 1993; Hayward et al., 1995) and polypeptides (Krimm and Bandekar, 1986; Noguti and Go, 1982), as well as by molecular dynamics simulations (Levy et al., 1985; Karplus and Petsko, 1990). These show that at frequencies below 400 cm^{-1}, the extended atom approximation is a useful simplification. This approach reduces the number of degrees of freedom by grouping the light hydrogens together with the heavy atoms to which they are attached, and treating the resulting group as though it were a point particle, with a mass appropriate for the group. At frequencies below 400 cm^{-1}, peptide backbone torsions and deformations result in relative motion of extended atom groups (e.g., CH, CH_2), and these modes are of a collective nature. Higher frequency modes involve predominantly stretching or bending of individual X-H bonds where X is a heavy atom. Examples of these high frequency oscillators, discussed below, are the amide modes V to II, lying between 400 and 1550 cm^{-1}, the in-plane and out-of-plane bending modes of aromatic ring hydrogens between 600 and 1600 cm^{-1}, and the methylene and methyl deformation modes between 950 and 1450 cm^{-1}. Recent neutron results seem to suggest a localized nature for the amide modes (Kearley et al., 1994). Experimental support for the collective nature of the modes below 400 cm^{-1} comes from the relative insensitivity of this region to hydrogen/deuterium (H/D) exchange in our $(PPG)_{10}$ sample, indicating that many hydrogens contribute to each low frequency mode.

Experimental dynamical structure factors

The factorization of $F_{inc}(Q, t)$ allows $S_{inc}(Q, \omega)$ to be written, in Eqs. A4–A7, in terms of a phonon expansion for the low frequency phonon modes of a chain of heavy beads, and a set of high frequency Einstein oscillators in the form of independent light particles bound harmonically to chain

elements (Warner et al., 1983). We identify the chain elements with extended atom groups, and the high frequency oscillators with protons of the groups. One-phonon creation processes dominate the inelastic spectrum at low energy transfer and low temperature, and we proceed on this assumption when discussing the low frequency region.

The experimental $S(Q, \omega)$, corrected for the Bose-Einstein thermal population factor for one-phonon scattering and labeled $S^{\#}(Q, \omega)$, are shown and compared in Figs. 3, 4, 5, and 8 for dry and hydrated collagen, deuterated and hydrogenous $(PPG)_{10}$, and PPII.

Collagen, $(PPG)_{10}$ and PPII all display a similar overall structure in the region below 400 cm^{-1}, although the details differ significantly. Two broad temperature and hydration-dependent bands are seen. We examined the temperature dependence of the bands in collagen by recording spectra from samples at 30 and 120 K in sequential runs (Fig. 6). A marked increase in intensity of the lowest lying band is apparent at the higher temperature.

We explored the effect of hydration for the collagen and $(PPG)_{10}$ samples. A difference spectrum of dry hydrogenous collagen and collagen hydrated to 25% with H_2O reveals additional intensity, in the hydrated sample, in the acoustic phonon region around 50 cm^{-1} (Fig. 5). This corresponds to an acoustic band observed in pure H_2O ice (Li and Ross, 1992). At 25% hydration, however, all the water in the collagen sample is closely associated with protein, and there is no pure ice. Nevertheless, in the interstices between collagen helices, packed in quasihexagonal arrangement, there are water molecules forming extended, hydrogen-bonded water chains and clusters (Hoeve and Tata, 1978). Such extended networks are capable of sustaining collective phonon excitations (White, 1976). We assign the 50 cm^{-1} peak in our difference spectrum to phonon excitations propagating through this interhelical water fraction. This assignment is supported by the absence of a similar 50 cm^{-1} peak in the difference spectrum between deuterated and hydrogenous $(PPG)_{10}$ (Fig. 4). The 6% of

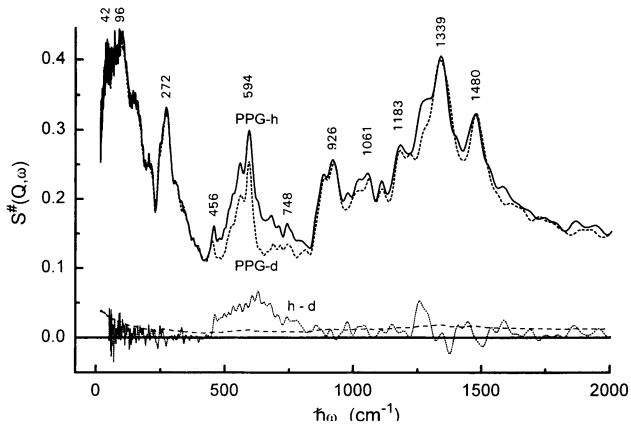

FIGURE 4 INS spectra, BE-corrected. $(PPG)_{10}$-h (——), and $(PPG)_{10}$-d (- - - -). Bottom curves: difference (h − d) (· · · · ·), and errors (inverse square root of no. of counts) (- - - -) (five-point FTF smoothed).

water present in our $(PPG)_{10}$ samples must be all tightly bound in water bridge sites on the peptide backbone. At this hydration level, water does not participate in any extended hydrogen-bonded network of water molecules, and so cannot sustain collective ice-like phonon excitations. Hence, as observed, no difference in the acoustic region is expected when H_2O is replaced by D_2O at 6% hydration. In contrast, D_2O exchange of the tightly bound water fraction in $(PPG)_{10}$ produces a marked loss of intensity in a broad band between 450 and 800 cm^{-1}, as revealed in the difference spectrum. This corresponds to a similar loss of intensity between 450 and 800 cm^{-1} on drying of 25% H_2O-hydrated collagen. The total intensity loss on passing from 25% H_2O hydrated to dry collagen is greater than that on passing from $(PPG)_{10}$-h to $(PPG)_{10}$-d. The detailed features of the two difference spectra are not identical. The collagen difference spectrum shows intensity extending to 1100 cm^{-1}, with further broad differences above 1500 cm^{-1}. Together these features suggest that both tightly bound and interhelical

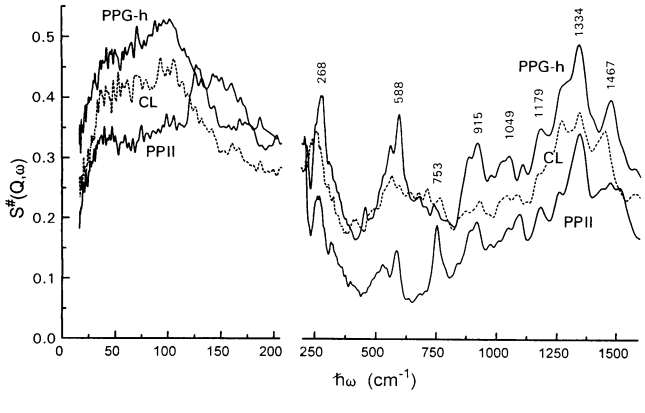

FIGURE 3 INS spectra, corrected for Bose-Einstein (BE) factor. $(PPG)_{10}$-h (PPG-h, upper ——, shifted by $\Delta S = +0.1$), H_2O-exchanged dry collagen (6% water, - - - -), and PPII (PPII, lower ——, shifted by $\Delta S = -0.1$). Slightly smoothed by a five-point Fourier transform filter (FTF).

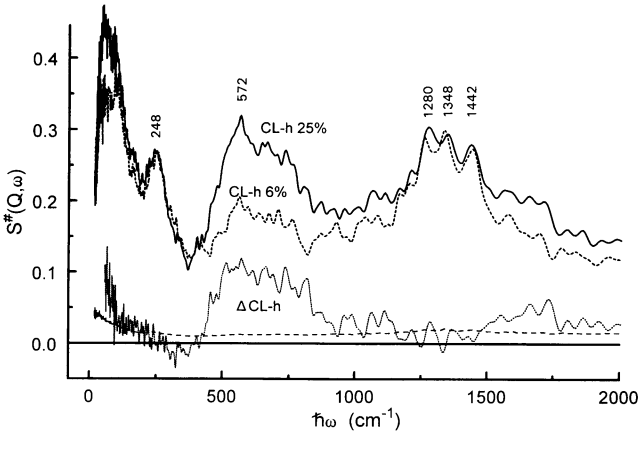

FIGURE 5 INS spectra, BE-corrected. H_2O-exchanged collagen, "dry" (6% water) (- - - -), and 25% hydrated (——). Bottom: difference (· · · · ·), errors (inverse square root of number of counts) (– – – –) (five-point FTF smoothed).

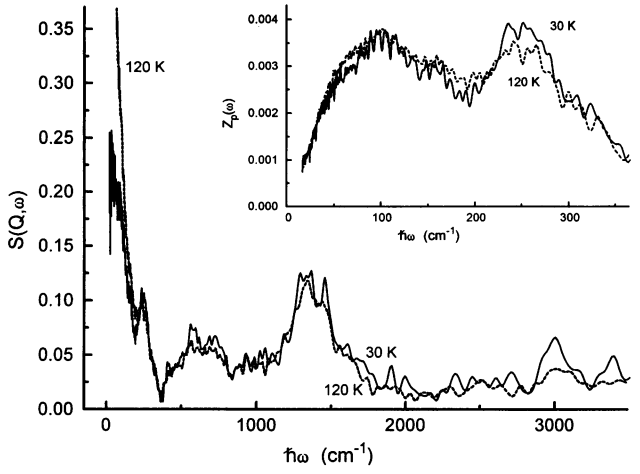

FIGURE 6 INS spectra from H_2O-exchanged dry collagen (6% water) at 30 K (——), and 120 K (- - - -). Insert: low frequency density of states, $Z_p(\omega)$, calculated from these spectra. All five-point FTF smoothed.

water contribute to the 450–800 cm^{-1} band, whereas only interhelical water contributes to the acoustic phonon band at 50 cm^{-1}. INS spectra from pure H_2O display a similar broad band of intensity in the intermediate energy transfer range, which is assigned to non-dispersive librational excitations in ice (Li and Ross, 1992). The overall shape resembles that of our difference spectra, with a sharp low frequency band edge followed by a broad maximum and a long high frequency tail. The low frequency edge appears at 540 cm^{-1}, and the band extends to 900 cm^{-1}. This frequency shift reflects the participation of protein groups hydrogen-bonded to water molecules in our samples. Water molecules tightly bound in water bridge sites in $(PPG)_{10}$ at 6% hydration appear to have similar librational dynamics to interhelical water molecules participating in the fully developed hydrogen-bonded network at 25% hydration.

Extraction of the density of states

One of the basic dynamical quantities characterizing a vibrating molecule is the distribution of vibrational frequencies $Z(\omega)$, known as the density of states. At low k_BT and for $Q \lesssim 1$ Å^{-1} (and hence low $\hbar\omega$ on TFXA), single-phonon terms are sufficient to describe the incoherent inelastic scattering response. A further useful approximation is to formulate the latter in terms of the phonon density of states (Smith, 1991). Since many hydrogen atoms are involved in each low frequency phonon mode, we make the approximation, in the low frequency region, of a uniform average weighting of $S_{inc}(Q, \omega)$ by the square of the atomic polarization vectors (see Appendix). Following earlier authors (Middendorf, 1984; Lovesey, 1984), we write:

$$S_{inc}(Q, \omega) = \exp\{-2W(Q)\}[n_{BE}(\omega) + 1] \times (\hbar Q^2/2M^*\omega)\, Z_p(\omega) \quad (5)$$

Here the first term is the Debye-Waller factor containing the atomic mean-square displacement along $\mathbf{Q}$, $\langle \mathbf{u}_p \cdot \mathbf{Q} \rangle^2$, and subscript ($p$) refers to the fact that our density of states function $Z_p(\omega)$ reflects the proton dynamics. Consistent with the use of an average weighting for the atomic polarization vectors, the exponent in the Debye-Waller factor is also averaged over the hydrogen atoms of the sample and is approximated by $\langle u_p^2 \rangle Q^2$. The effective mass of the oscillators is M^*, and $n_{BE}(\omega) = [\exp(\hbar\omega/k_BT) - 1]^{-1}$ is the Bose-Einstein (BE) thermal population factor.

To extract the relevant frequency distributions from our measured spectra at low energy transfer ($\hbar\omega \lesssim 350$ cm^{-1}), it is necessary to correct for the Debye-Waller as well as the Q^2/ω and thermal population factors. Given the relation between Q and ω imposed by the scattering kinematics of TFXA, the factor Q^2/ω in Eq. 5 is easy to evaluate from Eq. 3a. For the Debye-Waller factor we need $\langle u_p^2 \rangle$, the average mean-square displacement for the hydrogen atoms. We have determined this quantity from a series of high resolution quasi-elastic spectra for identical collagen samples oriented with their fiber axes perpendicular to the scattering plane, using the backscattering spectrometer IRIS at ISIS (Middendorf et al., 1990; H. D. Middendorf, R. L. Hayward, and J. P. Bradshaw, unpublished manuscript). At temperatures $T \lesssim 150$ K, these spectra consist of sets of elastic lines with a width of 0.13 cm^{-1} (FWHM) and total intensities that decrease linearly with Q^2. The low-temperature values for $\langle u_p^2 \rangle$ obtained in this way are in good agreement with neutron results for globular proteins (Doster et al., 1989; Martel, 1992). From the quasi-elastic data we get $\langle u_p^2 \rangle$ = 0.022 at 70 K, and 0.026 at 120 K. The $\langle u_p^2 \rangle$ displacements measured for collagen should be close to the corresponding values for our polypeptide models, and we have adopted them as reasonable estimates for these samples. Ordinary polymers give very similar values (Lynch et al., 1968). The resulting frequency distributions are shown in Fig. 6 for collagen at 30 and 120 K, and in Fig. 7 for PPII, dry collagen, and $(PPG)_{10}$.

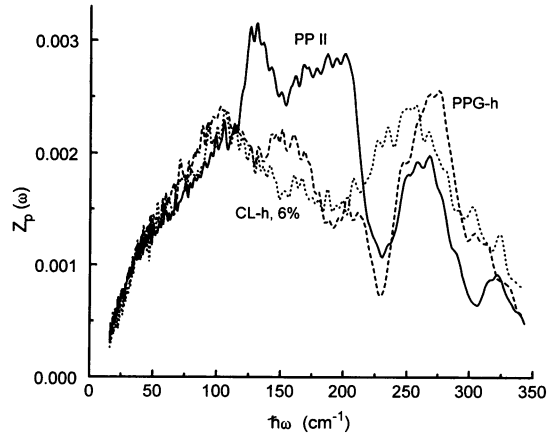

FIGURE 7 Hydrogen-weighted $Z_p(\omega)$. H_2O-exchanged dry collagen (6% water) (CL-h, ·····), $(PPG)_{10}$-h (PPG-h, - - - -), PPII (PPII, ——) (five-point FTF smoothed).

Up to $\hbar\omega \approx 400$ cm^{-1} the temperature dependence of the collagen spectra is in close accord with that predicted by Eq. 5. Correcting the intensity to allow for the thermal population factor and the temperature dependence of the Debye-Waller factor (as measured by quasi-elastic scattering) reveals a closely preserved structure in the density of states (Fig. 6). Anharmonicity is apparent in the second band, where methyl torsional fundamentals are expected near 240 cm^{-1}. Increasing temperature leads to a shift toward lower frequency, with loss of intensity from the fundamental peak, and increasing intensity near 200 cm^{-1}. Examination of the temperature dependence over a wider $\hbar\omega$ range is rendered problematic by the increasing influence of the Debye-Waller factor at high energy transfers and higher temperatures, and the complexity of its effects on localized group vibrations (Jobic and Lauter, 1988).

The general form of the low frequency region for collagen and $(PPG)_{10}$ is similar to the density of states calculated for PGII (Fanconi and Finegold, 1975). By analogy with these calculations, we assign the first broad band to dispersive phonon modes and the second to dispersive skeletal deformation modes. The structure of the first band in $(PPG)_{10}$ and in dry collagen are essentially identical (Figs. 3 and 7). Two submaxima are evident in both samples, at 45 and 110 cm^{-1}. The maximum at 45 cm^{-1} is better seen in Fig. 3, uncorrected for the Debye-Waller factor and the term Q^2/ω, because both these corrections tend to suppress the low frequency region below 100 cm^{-1}. Peaks at 40 and 110 cm^{-1} have been previously observed in collagen by INS at higher temperature (Berney et al., 1987). In calculations for PGII, the maximum due to longitudinal modes is seen at 13 cm^{-1} in the isolated molecule, but is displaced upward to 40 cm^{-1} when hydrogen-bonding to neighboring chains is taken into account. An inflection in the longitudinal mode branch is caused by softening of modes with wavevectors matching the pitch of the crystallographic helix, thereby producing a maximum in the density of states (Fanconi et al., 1971). These calculations are in broad agreement with INS spectra for PGII (Baron et al., 1989). We identify the 45 cm^{-1} peak in our collagen and $(PPG)_{10}$ spectra with this maximum for longitudinal acoustic modes in PGII-like chains hydrogen-bonded and supercoiled to form the collagen triple helix. The longitudinal acoustic phonon frequency in the polypeptide matches that of its associated interhelical ice shell, raising the possibility of coupling between solvent and polypeptide modes (White, 1975). At ordinary temperatures, the longitudinal acoustic mode velocity in collagen has been shown to vary with water content by optical Brillouin scattering (Cusack and Lees, 1984). Between 50 and 120 cm^{-1}, calculations for PGII reveal modes involving torsions of the peptide backbone (Dwivedi and Krimm, 1982), and a maximum in $Z_p(\omega)$ is expected in the region of 110 cm^{-1} (Fanconi and Finegold, 1975). We identify the band centered on 110 cm^{-1} in collagen and $(PPG)_{10}$ spectra with this maximum.

The remarkable features of the PPII spectrum in this region are the high and sharp torsional phonon band edge at 200 cm^{-1}, with a very intense peak at 130 cm^{-1} (Figs. 3 and 7). These features are in agreement with calculations of the phonon dispersion curves of PPII (Gupta et al., 1973). The high frequency of the band edge indicates a much stiffer effective force constant for torsional modes in PPII than in PGII, or even $(PPG)_{10}$ and collagen, despite their high content of proline. These spectral features presumably reflect the close-packed nature of neighboring pyrrolidine rings in PPII and the contribution of the rings to the peptide backbone stiffness. Stiffening of the peptide backbone as a consequence of pyrrolidine ring closure, as well as close packing of neighboring rings, have been evoked to explain the structural stability of PPII in solid state and solution, despite the absence of hydrogen bonds (Hopfinger, 1971). Similar proline/proline packing contributes to the stability of the triple-helical structure of $(PPG)_{10}$ (Bhatnagar et al., 1988). In $(PPG)_{10}$ and collagen, this packing arrangement is relieved at every third amino acid residue by the presence of glycine. Nevertheless, both dry collagen and $(PPG)_{10}$ spectra show additional features on the downward slope of the 110 cm^{-1} band edge, probably attributable to the imino residues (Fig. 7).

Deuteration of the $(PPG)_{10}$ amide hydrogen and the tightly bound water has little effect on the intensity of the bands below 400 cm^{-1}. The eigenvectors of the corresponding harmonic excitations must therefore involve the motion of many different hydrogen atoms, so that deuteration of the lone amide hydrogen and the single water molecule per tripeptide does not result in appreciable intensity changes. Such delocalized motion is in accordance with assignment to phonons involving relative motion of extended atom groups. The acoustic band, up to 50 cm^{-1}, represents relative translational motion of such groups. The backbone torsional band up to 100 cm^{-1} and the skeletal deformation band around 250 cm^{-1} represent relative rotational motion, resulting from deformations of the peptide backbone. These assignments are thus in agreement with the qualitative features of the PGII calculations (Fanconi and Finegold, 1975; Dwivedi and Krimm, 1982).

The calculated band gap at 200 cm^{-1} for PGII remains apparent, although not complete, in the spectra of the regular helices $(PPG)_{10}$ and PPII. For imino acid residues, less difference in frequency is expected for skeletal torsional modes, as opposed to skeletal deformation modes, given the influence of the imino pyrrolidine ring on backbone stiffness. This explains the incomplete nature of the 200 cm^{-1} band gap, despite the regularity of these helices. In dry collagen spectra the maximum of the skeletal deformation band appears at lower frequency, because methyl torsional modes, absent from $(PPG)_{10}$, contribute intensity near 240 cm^{-1}. The band gap is more nearly filled. Calculations of the frequencies of polypeptide skeletal torsion and deformation modes have revealed a significant variation with side chain type (Krimm and Bandekar, 1986). We attribute the filling of the band gap in collagen, at low temperature, to its complex amino acid sequence. As a first approximation, the sequence variation can be viewed as disorder in

bead mass and force constants of the perfectly regular $(PPG)_{10}$ type helix. Such disorder is expected to produce localization of vibrational energy (Van Zandt and Saxena, 1994), and modes where there are band gaps for the regular helix.

Proceeding from the experimental frequency distributions we extract an effective mass for the low frequency harmonic oscillators. For a normalized distribution $Z(\omega)$ of quantum harmonic oscillators at temperature T, the total mean-square displacement in one cartesian direction (Lovesey, 1984) is:

$$\langle u_p^2 \rangle = \int Z_p(\omega) \langle e^2(\omega) \rangle d\omega \qquad (6)$$

where

$$\langle e^2(\omega) \rangle = (\hbar/2\omega m(\omega)) \coth\{\hbar\omega/2k_BT\}$$

Here $m(\omega)$ is an effective mass for the harmonic oscillators, and depends on ω. Consistent with Eq. 5, we assume that m is approximately constant and equal to M* for all low frequency oscillators. This is not realistic for a complex heteropolymer. In particular, torsional modes of terminal groups (e.g., methyl groups) or librational modes of the idealized chain, may have significantly lower effective masses than those of translational modes. However, for our spectra the low frequency density of states for the dry samples is dominated by non-exchangeable hydrogens (attached to carbons), as is demonstrated by the correspondence between the $(PPG)_{10}$-h and $(PPG)_{10}$-d low frequency spectra. For the $(PPG)_{10}$ and PPII spectra there are no terminal methyl groups. Thus the effective mass extracted from the data gives a useful estimate of the mass of the heavy beads in this model. To derive this effective mass we need an independent determination of the total mean-square displacement, and this is provided by our quasi-elastic scattering experiments using IRIS. At low temperatures, moreover, the total mean-square displacement is dominated by the contribution of low frequency modes, and we therefore normalize our experimental density of states by the integrated intensity up to the minimum around 375 cm^{-1}. To calculate the total mean-square displacement, we first extended the measured spectra analytically from 16 to 0 cm^{-1} by fitting Debye spectra proportional to ω^2, and then integrated the product $Z_{p,375}(\omega)\langle e^2(\omega)\rangle$ from 0 to 375 cm^{-1}, where $Z_{p,375}(\omega)$ is the density of states normalized with respect to this energy range.

From this analysis we find that for an effective mass of 14.5 ± 3 a.m.u., the resulting mean-square displacements agree with values from our IRIS experiment over the temperature range 70 to 120 K (the error arising from the quasi-elastic experiment as well as from the assumption of constant effective mass up to $\hbar\omega \approx 375$ cm^{-1}). This effective mass is thus consistent with an idealized chain model utilizing extended atom groups as the beads of the chain, in which librational motions have an effective mass appreciably less than the atomic mass. Our data thus lend experimental support to the use of this approximation for the study of low frequency motions in proteins. Despite the continuing growth in speed and memory of computers, such approximations remain necessary for extending the length of molecular dynamics simulations into the biologically important ns–μs domain (Karplus and Petsko, 1990; Smith, 1991).

Multi-quanta scattering

We expect the harmonic nature of low temperature dynamics to be reflected in our spectra by intensity at energy transfers corresponding to combinations of low frequency dispersive phonons with high frequency group vibrations (Warner et al., 1983; Jobic and Lauter, 1988). Such intensity appears as phonon wings around each high frequency fundamental. Because of the relation between momentum transfer $\hbar Q$ and energy transfer $\hbar\omega$ imposed by the scattering kinematics of TFXA, we expect this effect to be most evident at intermediate $\hbar\omega$. Here Q is large enough to produce significant multiphonon scattering, but not so large as to reduce the scattering strongly through the Debye-Waller factor. In the spectrum of PPII, the intermediate energy transfer region shows strong peaks due to group vibrations. These are not clearly separated by regions of zero intensity, but instead show asymmetric broadening, maximal on the high frequency side. The mode at 745 cm^{-1} in the PPII spectrum displays this best. The next highest fundamental mode observed in IR (Isemura et al., 1968) or Raman (Smith et al., 1969) spectra of PPII is expected at 836 cm^{-1}, well above the region of asymmetric broadening of the 745 cm^{-1} mode. We attribute this asymmetric broadening to phonon wings. It is not possible to clearly identify this effect in $(PPG)_{10}$ or collagen, where many more fundamental modes are expected. At higher $\hbar\omega$, roughly above 1000 cm^{-1}, increasing multiquanta scattering contributes to a broad background, on which the peaks due to the harmonic fundamentals are superimposed.

Localized group vibrations: amide and high frequency modes

All collagen spectra are very complex in the high frequency region. Our assignments are based on comparison with the simpler neutron spectra of the model polypeptides PPII and $(PPG)_{10}$, and with published IR and Raman data for collagen and its models, along with normal coordinate analyses of polypeptide vibrational spectra. We contribute new IR data for $(PPG)_{10}$-h and $(PPG)_{10}$-d, the amide-deuterated isotopomer.

For the purpose of comparing spectra from different polypeptides containing a large molar fraction of proline, it is natural to use the spectral signature of proline as a reference intensity. All three types of sample (collagen, $(PPG)_{10}$ and PPII) show a strong peak at 1320 cm^{-1}, and another at 3000 cm^{-1}. A moderately strong peak has been observed at 1320 cm^{-1} in the IR (Isemura et al., 1968) and

Raman (Smith et al., 1969) spectra of polypeptides containing proline, and assigned to -CH_2 twist motion. The peak centered on 3000 cm^{-1} is the CH stretch band. We make these same assignments, and use these features to quantitatively relate our spectra.

Amides I, II, and III

Apart from the water libration band discussed above, there are several features in the difference spectrum between $(PPG)_{10}$-h and $(PPG)_{10}$-d that correspond to changes in the IR spectra on deuteration of the amide hydrogen. The most conspicuous change is a loss of intensity at 1250 cm^{-1}, with lesser changes at 1500 and 1550 cm^{-1}, and around 930 and 1020 cm^{-1} in the $(PPG)_{10}$-d spectra (Fig. 4). In IR spectra a peak at 1550 cm^{-1} and another at 1250 cm^{-1} are markedly reduced by deuteration (see Table 1), as are two lesser peaks at 920 and 1029 cm^{-1}. The peaks at 1550 cm^{-1} and 1250 cm^{-1} are identified, in normal coordinate analyses of PGII (Dwivedi and Krimm, 1982), polyalanine (Fanconi et al., 1971), and the peptide bond model compound *N*-methylacetamide (Fillaux et al., 1993; Krimm and Bandekar, 1986), with in-plane bending of the amide hydrogen, coupled with stretching of the CN bond (amides II and III). This assignment agrees with the effects of deuteration on our $(PPG)_{10}$ spectra. Clearly the formation of the peptide bond with an imino acid, rather than an amino acid, and the results of helix supercoiling, do not greatly perturb these vibrational frequencies. As expected the peaks at 1250 and 1550 cm^{-1} are absent from the PPII spectra, where no amide hydrogens are present. Relative to the peak at 1320 cm^{-1}, both amide II and amide III are stronger in dry collagen spectra than in $(PPG)_{10}$, as expected from the higher ratio of amino to imino acids in collagen. The origin of the spectral changes with deuteration in $(PPG)_{10}$ near 925 and 1025 cm^{-1} is much less clear, as there are no amide modes expected in this region. It may be that these changes are related to excitations involving the tightly bound water molecules.

Amide I is expected to be weak in INS spectra if it involves little hydrogen motion. We observe no significant intensity at 1650 cm^{-1}, where Raman and IR spectra have revealed the amide I peak in collagen (Brodsky-Doyle et al., 1975; Frushour and Koenig, 1975) and $(PPG)_{10}$ (Diem et al., 1984). This supports the assignment of amide I to C═O stretch, with little hydrogen motion.

Amide V, skeletal modes, and effects of higher-order molecular structure

In PGII (Dwivedi and Krimm, 1982), polyalanine (Fanconi et al., 1971), and the hydrogen-bonded crystals of the peptide bond model compounds *N*-methylacetamide (Fillaux et al., 1993; Krimm and Bandekar, 1986) and acetanilide (Barthés et al., 1992), the NH out-of-plane mode, amide V, mixed with C═O in-plane bend, appears at 750 cm^{-1}. This is typical for a hydrogen-bonded amide hydrogen. A mode involving C═O in-plane bend mixed with skeletal deformation is expected at 707 cm^{-1}. In INS spectra from PGII, a strong peak is present in this region (Baron et al., 1989). There is also a strong peak in our PPII neutron spectrum at 745 cm^{-1} (Fig. 3), corresponding to a very weak peak in the IR spectrum (Isemura et al., 1968) and a moderate peak in the Raman spectrum (Smith et al., 1969). Normal coordinate analysis has assigned this feature to C═O in-plane bending along with in-plane bending of the backbone skeleton and deformation of the proline ring (Gupta et al., 1973). The remarkable feature of our triple-helical $(PPG)_{10}$-h and $(PPG)_{10}$-d INS spectra is the absence of any corresponding strong peak in the region between 650 and 820 cm^{-1} (Fig. 4). Neither an amide V mode nor a C═O in-plane bending mode is observed in this region. On the other hand, when compared with PPII, excess intensity in the spectra of $(PPG)_{10}$-h is apparent in the strong doublet peak at 555 and 590 cm^{-1}. The shape of this peak does not change in $(PPG)_{10}$-d, although the overall intensity in this region changes as a result of intensity arising from the underlying water librational band. An effect of triple-helix formation on high frequency modes of the peptide linkage has been previously observed in Raman studies comparing the tripeptide PPG with $(PPG)_{10}$, and ascribed to secondary structure formation. The effect of helix-sheet transitions or peptide *cis/trans* isomerization on skeletal modes is well recognized (Krimm and Bandekar, 1986). The dramatic change we observe in the amide V region on passing from the left-handed helical arrangement of PPII and PGII to the supercoiled triple-helical $(PPG)_{10}$ structure must be attributed instead to the tertiary structure.

The effect of triple-helical supercoiling is to shift the amide V mode of the Gly-Pro linkage, together with skeletal deformation and C═O in-plane bending modes of the Pro-Pro linkages, downward to the region of 590 cm^{-1}. The NH out-of-plane bending mode is not clearly identified by H/D exchange in the triple-helical peptides because of the background due to water libration. The effect may be mediated by supercoiling distortion of the intra-triple-strand hydrogen bond and the backbone dihedral angles in $(PPG)_{10}$. In the crystal structure of $(PPG)_{10}$, the local distortions from standard values of the backbone dihedral angles, bond angles, and endocyclic ring conformation angles are only 7, 2, and 5 degrees, respectively, and they vary with the detail of the molecular model (Okuyama et al., 1981). The intra-triple-strand hydrogen bond, between glycine NH on one chain and proline CO on a neighboring supercoiled chain, also varies in length and N-H . . . O angle with the molecular conformation (Yonath and Traub, 1969; Okuyama et al., 1981; Bhatnagar et al., 1988). The equivalent hydrogen bond and backbone geometries in models of collagen also vary with the details of the molecular structure (Fraser et al., 1983). Theoretical normal mode analyses have predicted significant effects of minor angle variation and hydrogen bonding on amide V modes (Krimm and Bandekar, 1986). Our observation of a substantial spectral effect of the subtle supercoiling distortion raises the question of coupling between low frequency modes and high frequency peptide backbone modes. Low frequency dispersive modes can sig-

nificantly alter local supercoiling and hydrogen bond length. Such anharmonic coupling may be an important mechanism of energy transport in biological systems (Scott, 1992), and amide V has been recently identified as a markedly anharmonic mode, and a candidate for such coupling, in acetanilide (Barthés et al., 1992). In polyproline, a moderately strong IR band at 670 cm^{-1} is characteristic of the left-handed PPII arrangement and is assigned by normal mode calculation to a mixture of skeletal stretch with pyrrolidine ring in-plane deformation (Gupta et al., 1973). This mode is weak in our PPII spectra, indicating little hydrogen atom motion in the mode (Fig. 3).

Collagen versus PPII and $(PPG)_{10}$

Compared with $(PPG)_{10}$, the dry collagen spectra reveal significantly more intensity in the 600–800 cm^{-1} region (Fig. 3). Contributions from amino acid side chains other than pyrrolidine rings can be expected in this region. Out-of-plane bending modes for side chain NH groups contribute to the collagen spectra but are absent from $(PPG)_{10}$. The contribution of phenylalanine and tyrosine ring modes will be small because of the low abundance of these amino acids in collagen, but librational water modes from the 6% H_2O fraction will produce a broad background. Results from TFXA spectra and detailed molecular dynamics simulations for acetanilide (Hayward et al., 1995) give some insight into the nature of the complex bands in the amide V region, in particular with respect to splitting due to mixing of NH and phenyl CH out-of-plane bending modes and their interaction with peptide deformation modes. In their Raman study of solution samples at room temperatures, Diem et al. (1984) found excellent agreement between collagen and $(PPG)_{10}$ spectra in the 700-1000 cm^{-1} region. Our results show substantial differences, highlighting the sensitivity to hydrogen motions and the complementarity of these techniques. A quantitative analysis must await spectral simulations for $(PPG)_{10}$-h and $(PPG)_{10}$-d.

Relative to the band intensities observed for dry collagen between 500 and 800 cm^{-1}, the CH_2 twist and wag modes of the pyrrolidine ring at 1320 and 1450 cm^{-1} are stronger by almost a factor of 2. These modes are due to the relatively high abundance of the imino acids, and the whole 1200–1500 cm^{-1} region is very similar in structure and intensity for all three samples, i.e., dry collagen, $(PPG)_{10}$-h and PPII. The imide II band between 1445 and 1485 cm^{-1} has been of recent interest in resonance Raman studies of X-Pro or Pro-Pro *cis/trans* isomerization (X = any amino acid) and imino hydrogen bonding (Tageuchi and Harada, 1990). This band is another example of a high frequency mode affected by a major change in backbone conformation. The band is not seen in our spectra; it seems to be obscured by the very strong pyrrolidine ring CH_2 deformation band at 1450 cm^{-1} (Figs. 3 and 8). This illustrates a difficulty in interpreting neutron spectra, where modes of particular interest may involve little hydrogen motion. Selective deuteration of the pyrrolidine ring methylene groups might in the future allow observation of the imide II band. In the collagen spectra, additional intensity around 1435 cm^{-1} arises from methyl group deformations. Methyl modes also contribute intensity to the collagen spectra between 1050 and 1070 cm^{-1}. These assignments are confirmed by calculation and INS data for the model compounds *N*-methylacetamide (Fillaux et al., 1993) and acetanilide (Barthés et al., 1992; Hayward et al., 1995).

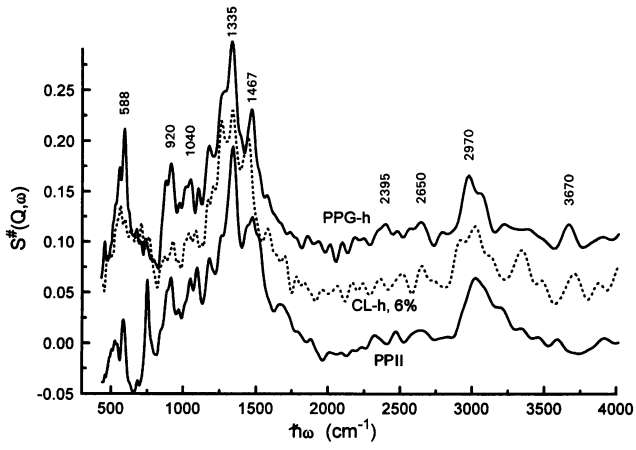

FIGURE 8 BE-corrected INS spectra, intermediate and high frequency regions. $(PPG)_{10}$-h (PPG-h, upper ——, shifted by $\Delta S = +0.05$), H_2O-exchanged dry collagen (6% water, · · · · ·), and PPII (PPII, lower ——, shifted by $\Delta S = -0.05$).

Several features common to PPII and $(PPG)_{10}$, notably at 920, 1040, 1100, and 1170 cm^{-1}, are also apparent in the collagen spectra, again reflecting the high content of imino acids (Figs. 4–7). Calculations attribute the modes at 920 and 1040 cm^{-1} to pyrrolidine ring stretch modes, and those at 1100 and 1170 cm^{-1} to mixed ring stretch and ring methylene modes (Gupta et al., 1973; Lagant et al., 1983). The ring stretching modes at 1250 to 1260 cm^{-1}, seen in the PPII and $(PPG)_{10}$-d spectra, are obscured by the amide III mode in $(PPG)_{10}$ and collagen spectra (Figs. 3 and 4).

Centered on 3000 cm^{-1}, a strong CH stretch band is seen in all samples (Fig. 8). The resolution of TFXA at the highest $\hbar\omega$ is only $\approx$100 cm^{-1}, and the effect of the Debye-Waller factor is strong, as is evident from the substantial reduction in intensity of this band at 120 K. These facts prevent the direct observation of splitting of the NH stretching modes, amides A and B, although a band attributable to NH stretch centered at 3300 cm^{-1} is apparent in collagen spectra (Fig. 8). The same band is not well distinguished in $(PPG)_{10}$ because of the much lower molar content of NH groups. Again, selective deuteration of CH groups is likely to reveal these modes.

CONCLUSIONS AND OUTLOOK

We have presented and discussed neutron spectra from collagen, the most important fibrous protein. We have interpreted the data with reference to analytical theories of

scattering from complex polymers and with the help of parallel neutron and IR measurements on two closely related synthetic polypeptides.

From an experimental point of view, the neutron spectra obtained are the first from any natural protein extending from the low frequency acoustic phonon region up to the highest bond-stretching modes. Earlier neutron work on fibrous and globular biomolecules was restricted with respect to both frequency range and resolution. Cold-neutron time-of-flight spectrometers covered only the low frequency phonon region in upscattering, with sharply deteriorating intensity and resolution beyond a few 100 cm^{-1}, and crystal filter spectrometers provided spectra up to $\approx$1200 cm^{-1} with poor resolution. Developments in pulsed neutron techniques have now allowed us to probe a frequency range of more than two decades with a resolution that is still inferior to IR and Raman spectroscopy, but sufficiently fine to reveal much spectral detail. This new spectral information relates primarily to the dynamics of hydrogens, protonated groups, and closely associated water. In combination with quasi-elastic neutron scattering techniques (Middendorf, 1992, 1995; Middendorf et al., 1994), it is feasible to probe hydration processes, biopolymer-water coupling, and intrinsic biopolymer modes over scale lengths from 1 to 100 A, with the capability, not easily accomplished by optical techniques, of varying the scattering contrast between constituents of a heterogeneous system.

There are, broadly, two avenues for further exploiting this type of INS data from complex biopolymers. The first, as we have demonstrated, is to focus on those features that complement information derived from optical techniques, and on density of states functions relating to basic thermodynamic properties. In particular, we have observed a dramatic shift of the amide V mode in triple-helical polymers, indicating a marked effect of supercoiling on the dynamics of the hydrogen bond. We have used density of states information to extract an effective mass for the low frequency oscillators, which suggests that the extended atom approximation will be a useful simplification for calculations of protein dynamics. Secondly, the analytical relationship between neutron $S(Q, \omega)$ data and fundamental space-time correlations at the atomic level, opens up the possibility of direct comparison with results from molecular dynamics (MD) simulations. The potential of INS to provide experimental constraints on calculations of the low frequency dynamics of globular proteins has been demonstrated (Smith, 1991). While much of the functional interest in globular proteins relates to the region of collective relaxational and anharmonic excitations below a few 100 cm^{-1}, recent work on vibrational energy transport mechanisms has focused on the coupling of low and high frequency modes in fibrous as well as globular proteins. Such mode-coupling mechanisms are potentially significant for the function of enzymes that need to transport localized "packets" of energy, with minimal losses, between active sites that may be separated by appreciable distances (Scott, 1992). The utility of simulations to study mode-coupling mechanisms will rest on the accurate description of high as well as low frequency vibrational modes. MD simulations are performed by following the trajectories of all atoms over the entire time domain from a few fs up to nearly 1 ns, thus providing essentially the full van Hove function $G(r, t)$ and producing spectral information from a few 10^3 cm^{-1} down to values well below 1 cm^{-1} (Karplus and Petsko, 1990; Smith, 1991). Our neutron experimental work opens up the whole vibrational spectral region from 20 to 4000 cm^{-1}, with improved resolution, providing further stringent tests for the parameters and assumptions entering into simulations of biomolecular dynamics. However, our data are collected at low temperatures where broadening effects due to diffusive processes are negligible and where the intrinsic resolution of the spectra is not degraded by multiphonon scattering. This restricts the dynamics we probe to the harmonic region of the potential energy surface, and our data will be useful primarily in this region for improving the parametrization of MD potential energy functions. Furthermore, our data lend support to the validity of the extended atom approximation, which treats the high frequency localized oscillators as harmonic oscillators, essentially independent of the collective modes at low frequencies where anharmonic effects are more prevalent.

Exploiting the technique of contrast variation, we have extracted difference spectra related to the dynamics of two different populations of protein-associated water. Such spectra can provide an important test of calculations of, especially, the high frequency harmonic modes of tightly bound water molecules. These high frequency modes reflect the hydrogen-bonding parameters of waters occupying water bridge sites, information of great interest for understanding the functional role of the primary hydration shell of proteins.

APPENDIX

The dynamic structure factors $S_{inc/coh}(\mathbf{Q},\omega)$ and the nuclear trajectories $\mathbf{R}_\alpha(t)$ are directly related through $\omega \leftrightarrow t$ Fourier transforms of Q-dependent time correlation functions, the so-called "intermediate" scattering functions (Berney and Yip, 1980; Windsor, 1981; Lovesey, 1984). These are given by

$$\mathbf{F}_{coh}(\mathbf{Q}, t) = \mathbf{FT}\{S_{coh}(Q, \omega)\} = (1/N) \sum_{\alpha,\beta} \langle \exp\{ - i\mathbf{Q} \cdot \mathbf{R}_\alpha(0)\} \exp\{i\mathbf{Q} \cdot \mathbf{R}_\beta(t)\}\rangle \quad \text{(A1)}$$

together with a similar function $F_{inc}(\mathbf{Q}, t)$ for which only the diagonal terms $\alpha = \beta$ are summed ($\alpha, \beta = 1 \ldots N$). Here and below the brackets $\langle\rangle$ denote thermal ensemble averages. Eq. A1 relates to coherent scattering, since it covers all pair correlations including the "self" terms $\alpha = \beta$; for $F_{inc}(\mathbf{Q}, t)$ the single-particle correlations described by $\alpha = \beta$ are sufficient. A further Fourier transformation, with respect to the conjugate variables $Q \leftrightarrow r$ instead of $\omega \leftrightarrow t$, leads from $F_{inc}(\mathbf{Q}, t)$ and $F_{coh}(\mathbf{Q}, t)$ to the van Hove space-time correlation functions $G_s(\mathbf{r}, t)$ and $G(\mathbf{r}, t)$, respectively (Berney and Yip, 1980; Lovesey, 1984).

For a hierarchically organized macromolecular structure, now, a useful approximation is to split $\mathbf{R}_\alpha(t)$ into components due to restricted diffusive motions, dispersive phonon modes (including low frequency acoustic

modes, or LAM), and localized (nondispersive) group vibrations. For the temperatures of interest in the present context, and at frequencies $>10^{11}$ Hz or 3 cm^{-1}, the spectral contribution from restricted diffusive motions (which would give rise to quasi-elastic scattering with $|\hbar\omega| \ll E_t$) is zero or negligibly small. $\mathbf{R}_\alpha(t)$ may therefore be expressed in terms of an equilibrium position and a displacement from equilibrium. The mean-square value of the latter is split into a term due to phonons ($\mathbf{u}_\alpha$) and one due to group vibrations ($\mathbf{v}_\alpha$):

$$\mathbf{R}_\alpha(t) = \mathbf{R}_\alpha^\circ + \delta\mathbf{R}_\alpha(t); \quad \langle(\delta\mathbf{R}_\alpha(t))^2\rangle = \langle u_\alpha^2\rangle + \langle v_\alpha^2\rangle \qquad \text{(A2)}$$

The distinction between low frequency phonon modes and localized group excitations at higher frequencies amounts to a time scale separation which is equivalent to a factorization of the respective intermediate scattering functions. For dominant incoherent scattering from the protons, we need consider only $F_{inc}(\mathbf{Q}, t)$ and write:

$$F_{inc}(\mathbf{Q}, t) = (1/N_l) \sum_l \langle \exp\{-i\mathbf{Q}\cdot\mathbf{u}_l(0)\} \exp\{i\mathbf{Q}\cdot\mathbf{u}_l(t)\}\rangle$$

$$\times (1/N_j) \sum_j \langle \exp\{-i\mathbf{Q}\cdot\mathbf{v}_j(0)\} \exp\{i\mathbf{Q}\cdot\mathbf{v}_j(t)\}\rangle \qquad \text{(A3)}$$

where $l = 1 \ldots N_l$ labels the chain elements or "beads," and $j = 1 \ldots N_j$ the protons in a chain element. In the frequency domain, this factorization corresponds to a convolution product,

$$S_{inc}(\mathbf{Q}, \omega) = S_{inc}^{L}(\mathbf{Q}, \omega) \otimes S_{inc}^{J}(\mathbf{Q}, \omega) \qquad \text{(A4)}$$

We now write S_{inc}^{L} in terms of a phonon expansion for the low frequency modes of a chain of heavy beads, and reduce S_{inc}^{J} to a set of Einstein oscillators (Warner et al., 1983; Jobic and Lauter, 1988):

High frequency oscillators

For independent light particles (protons of mass m_p) bound harmonically to chain elements, the basic result is

$$S_{inc}^{J}(\mathbf{Q}, \omega) = \sum_j \exp(-\langle v_j^2\rangle Q^2) \prod_\lambda \Big[\sum_{n_\lambda} \exp\{n_\lambda \hbar\omega_\lambda / 2k_B T\} \qquad \text{(A5)}$$

$$\times I_{n_\lambda}(\hbar|\mathbf{Q}\cdot\mathbf{e}_\lambda^j|^2/2m_p\omega_\lambda \sinh\{\hbar\omega_\lambda/2k_BT\}) \Big] \delta(\omega - \sum_\lambda n_\lambda\omega_\lambda)$$

Here $\mathbf{e}_\lambda^j$ is the normalized polarization vector for proton j in the mode λ, and n_λ the number of quanta of energy $\hbar\omega_\lambda$ transferred in the scattering process ($n_\lambda > 0$ for neutron energy loss, $n_\lambda < 0$ for energy gain). The first exponential is the high frequency Debye-Waller factor of proton j, due to displacements v_j, and $I_{n\lambda}$ denotes the n_λth-order modified Bessel function. It is seen that the high frequency spectrum consists of a series of δ-function spikes at frequencies where the energy change $\hbar\omega$ experienced by scattered neutrons equals an allowed transition or combination of transitions. At low temperatures ($4k_BT < \hbar\omega_\lambda$), and for the Q,ω-relation given by Eq. 3, we have $x < 0.3$ so that the leading term in the expansion of $I_{n\lambda}(x)$ is sufficient. The dominant downscattering process is characterized by the fundamental $n_\lambda = 1$; Eq. A5 then reduces to

$$S_{inc}^{J}(\mathbf{Q}, \omega) = \sum_j \exp(-\langle v_j^2\rangle Q^2)(n_{BE} + 1)$$

$$\times (\hbar|\mathbf{Q}\cdot\mathbf{e}^j|^2/2m_p\omega_\lambda)\, \delta(\omega - \omega_\lambda) \qquad \text{(A6)}$$

where $n_{BE} = [\exp(\hbar\omega_\lambda/k_BT) - 1]^{-1}$ is the Bose-Einstein population factor.

Phonon expansion

A full analysis requires calculated or measured dispersion curves $\omega_\nu(\mathbf{q})$ for all low frequency chain modes ($\mathbf{q}$ = phonon momentum; ν = branch index). For incoherent scattering, the main aim is to extract $Z_p(\omega)$ from the one-phonon scattering (Lovesey, 1984). At low temperatures and modest values of Q, subject to the assumption of harmonic excitations and appropriate averaging of polarization vectors (see main text), a phonon expansion for the measured spectra may be written in the form (Suck and Rudin, 1983)

$$(\hbar k_o/Nk) d^2\sigma/d\Omega dE = \exp(-\langle u_p^2\rangle Q^2) \sum_{n=1}^{\infty} [f_n(\omega)/n!]$$

$$\times (\hbar^2 Q^2/2M^*)^n \qquad \text{(A7)}$$

where

$$f_n(\omega) = \int_{-\infty}^{\infty} f_{n-1}(\omega') f_1(\omega - \omega') d\omega' \quad (\text{for } n > 1),$$

and

$$f_1(\omega) = (n_{BE} + 1) Z_p(\omega)/\hbar\omega\,.$$

This is an iterative approach that enables the multi-phonon contributions f_n ($n > 1$) to be separated from measured spectra, with $Z_p(\omega)$ as the remaining one-phonon part.

We thank the ISIS Facility, Rutherford Appleton Laboratory, Chilton, U.K., and the Institut Laue-Langevin, Grenoble, France, for the use of neutron facilities. We are greatly indebted to J. Tomkinson and A. V. Belushkin for much advice on data analysis, and for assistance during experiments.

This work was supported by the Wellcome Trust and the Sir Edward Abrahams Cephalosporin Fund.

REFERENCES

Arnott, S., and S. D. Dover. 1968. The structure of poly-L-proline II. *Acta Cryst.* B24:599–601.

Baron, M. H., F. Fillaux, and J. Tomkinson. 1989. Inelastic neutron scattering study of the proton dynamics in polyglycine I and II. *In* Spectroscopy of Biological Molecules: State of the Art. Esculapo, Bologna, Italy. 83–129.

Barthés, M., J. Eckert, S. W. Johnson, J. Moret, B. I. Swanson, and C. J. Unkefer. 1992. Anomalous vibrational modes in acetanilide as studied by inelastic neutron scattering. *J. Physique I.* 2:1929–1939.

Bella, J., M. Eaton, B. Brodsky, and H. M. Berman. 1994. Crystal and molecular structure of a collagen like peptide at 1.9 A resolution. *Science (Wash. DC).* 266:75–79.

Bellissent-Funel, M.-C., J. Teixeira, S. H. Chen, B. Dorner, H. D. Middendorf, and H. L. Crespi. 1989. Low frequency collective modes in dry and hydrated proteins. *Biophys. J.* 56:713–716.

Berney, C. V., V. Renugopalakrishnan, and R. S. Bhatnagar. 1987. Collagen: an inelastic neutron scattering study of low frequency vibrational modes. *Biophys. J.* 52:343–345.

Berney, C. V., and S. Yip. 1980. Inelastic neutron scattering spectroscopy. *In* Methods of Experimental Physics, Vol. 16A. R. A. Fava, editor. Academic Press, New York. 205–240.

Bhatnagar, R. S., N. Pattabiraman, K. R. Sorenson, R. Langridge, R. D. MacElroy, and V. Renugopalakrishnan. 1988. Inter-chain proline: proline contacts contribute to the stability of the triple-helical conformation. *J. Biomol. Struct. Dyn.* 6:223–233.

Bradshaw, J., A. Miller, S. T. Robertson, and H. D. Middendorf. 1992. High-resolution vibrational neutron spectra of collagen. *Physica. B* 180/181:776–779.

Brodsky-Doyle, B., E. G. Bendit, and E. R. Blout. 1975. Infrared spectroscopy of collagen and collagen-like polypeptides. *Biopolymers.* 14: 937–957.

Chen, S.-H., J. D. Jorgensen, and C. V. Berney. 1978. Neutron molecular spectroscopy using a white beam time-of-flight spectrometer. *J. Chem. Phys.* 68:209–215.

Crick, F. H. C., and A. Rich. 1955. The structure of polyglycine II. *Nature (Lond.).* 176:780–781.

Cusack, S., and S. Lees. 1984. Variation of longitudinal acoustic velocity with water content in rat-tail tendon fibers. *Biopolymers.* 23:337–351.

Diem, M., R. S. Bhatnagar, M. E. Druyan, and V. Renugopalakrishnan. 1984. Solution phase Raman spectroscopic studies on synthetic collagen analogs: prolyl-prolyl-glycine and (prolyl-prolyl-glycine)$_{10}$. *Biopolymers.* 23:2955–2961.

Doster, W., S. Cusack, and W. Petry. 1989. Dynamical transition of myoglobin as revealed by inelastic neutron scattering. *Nature (Lond.).* 337:754–756.

Dwivedi, A. M., and S. Krimm. 1982. Vibrational analysis of peptides, polypeptides and proteins. XV. Crystalline polyglycine II. *Biopolymers.* 21:2377–2397.

Fanconi, B., and L. Finegold. 1975. Vibrational states of the biopolymer polyglycine II: theory and experiment. *Science (Wash. DC).* 190: 458–459.

Fanconi, B., E. W. Small, and W. L. Peticolas. 1971. Phonon dispersion curves and normal coordinate analysis of poly-L-alanine. *Biopolymers.* 10:1277–1298.

Fillaux, F., J. P. Fontaine, M. H. Baron, G. Kearley, and J. Tomkinson. 1993. Inelastic neutron-scattering study of the proton dynamics in *N*-methyl acetamide at 20 K. *Chem. Phys.* 176:249–278.

Fraser, R. D. B., T. P. MacRae, and A. Miller. 1987. Molecular packing in type I collagen fibrils. *J. Mol. Biol.* 193:115–125.

Fraser, R. D. B., T. P. MacRae, A. Miller, and E. Suzuki. 1983. Molecular conformation and packing in collagen fibrils. *J. Mol. Biol.* 167:497–521.

Frushour, B. G., and J. L. Koenig. 1975. Raman scattering of collagen, gelatin, and elastin. *Biopolymers.* 14:379–391.

Grigera, J. R., and H. J. C. Berendsen. 1979. The molecular details of collagen hydration. *Biopolymers.* 18:47–57.

Grimm, H., H. Stiller, C. F. Majkrzak, A. Rupprecht, and U. Dahlborg. 1987. Observation of acoustic umklapp phonons in water stabilized DNA. *Phys. Rev. Lett.* 59:1780–1783.

Gupta, V. D., R. D. Singh, and A. M. Dwivedi. 1973. Vibrational spectra and dispersion curves of poly-L-proline II chains. *Biopolymers.* 12: 1377–1385.

Hayward, R. L., H. D. Middendorf, U. Wanderlingh, and J. C. Smith. 1995. Dynamics of crystalline acetanilide: analysis using neutron scattering and computer simulation. *J. Chem. Phys.* 102:5525–5541.

Hoeve, C. A. J., and A. S. Tata. 1978. The structure of water absorbed in collagen. *J. Phys. Chem.* 82:1661–1663.

Hopfinger, A. J. 1971. The lattice energetics of some polypeptide chains. *Biopolymers.* 10:1299–1315.

Isemura, T., H. Okabayashi, and S. Sakakibara. 1968. Steric structure of L-proline oligopeptides. I. Infrared absorption spectra of the oligopeptides and poly-L-proline. *Biopolymers.* 6:307–321.

Jobic, H., and H. J. Lauter. 1988. Calculation of the effect of the Debye-Waller factor on the intensity of molecular modes measured by neutron inelastic scattering. *J. Chem. Phys.* 88:5450–5457.

Jones, E. Y. 1985. Structural and dynamic studies on biological macromolecules. Ph.D. thesis. University of Oxford, Oxford, UK. 169 pp.

Kadler, K. 1994. Extracellular matrix 1: fibril-forming collagens. *Protein Profile.* 1:519–612.

Karplus, M., and G. Petsko. 1990. Molecular dynamics simulations in biology. *Nature (Lond.).* 347:631–639.

Kearley, G. J., F. Fillaux, M.-H. Baron, S. Bennington, and J. Tomkinson. 1994. A new look at proton transfer dynamics along hydrogen bonds in amides and peptides. *Science (Wash. DC).* 264:1285–1289.

Krimm, S., and J. Bandekar. 1986. Vibrational spectroscopy and conformation of peptides, polypeptides, and proteins. *Adv. Protein Chem.* 38:181–364.

Lagant, P., M. H. Loucheux-Lefebvre, J. P. Huvennne, G. Vergoten, G. Fleury, and P. Legrand. 1983. Raman spectra and normal vibrations of dipeptides. II. Glycyl-L-proline. *Biopolymers.* 22:1285–1300.

Levy, R. M., R. P. Sheridan, J. W. Keepers, G. S. Dubey, S. Swaminathan, and M. Karplus. 1985. Molecular dynamics of myoglobin at 298 K. *Biophys. J.* 48:509–518.

Li, J-C., and D. K. Ross. 1992. Neutron scattering studies of ice dynamics. *In* Physics and Chemistry of Ice, Parts I and II. N. Maeno and T. Hondoph, editors. Hokaido University Press, Sapporo, Japan. 27–42.

Lovesey, S. 1984. Theory of neutron scattering from condensed matter. Vol. 1. Oxford University Press, Oxford, UK. 329 pp.

Lynch, J. E., G. C. Summerfield, L. A. Feldkamp, and J. S. King. 1968. Neutron scattering in normal and deuterated polyethylene. *J. Chem. Phys.* 48:912–918.

Martel, P. 1992. Biophysical aspects of neutron scattering of vibrational modes in proteins. *Prog. Biophys. Mol. Biol.* 57:129–179.

Middendorf, H. D. 1984. Biophysical applications of quasi-elastic and inelastic neutron scattering. *Annu. Rev. Biophys. Bioeng.* 13: 425–451.

Middendorf, H. D. 1992. Neutron studies of the dynamics of globular proteins. *Physica.* B182:415–420.

Middendorf, H. D. 1995. Neutron scattering techniques for the investigation of proton transport phenomena. *Solid State Ionics.* 77:265–274.

Middendorf, H. D., J. Bradshaw, and A. Miller. 1990. Report on experiments RB748 and RB749. *ISIS Annu. Rep.* A220.

Middendorf, H. D., D. DiCola, F. Cavatorta, A. Deriu, and C. J. Carlile. 1994. Water dynamics in charged and uncharged polysaccharides gels by quasi-elastic neutron scattering. *Biophys. Chem.* 47:145–153.

Middendorf, H. D., and J. T. Randall. 1985. Neutron spectroscopy and protein dynamics. *In* Structure and Motion: Membranes, Nucleic Acids and Proteins. E. Clementi, G. Corongiu, M. H. Sarma, and R. H. Sarma, editors. Adenine Press, New York. 219–241.

Miller, A. 1984. Collagen: the organic matrix of bone. *Philos. Trans. R. Soc. Lond. B.* 304:455–477.

Noguti, T., and N. Go. 1982. Collective variable description of small-amplitude conformational fluctuations in a globular protein. *Nature (Lond.).* 296:776–778.

Okuyama, K., K. Okuyama, S. Arnott, M. Takayanagi, and M. Kakudo. 1981. Crystal and molecular structure of a collagen-like polypeptide (Pro-Pro-Gly)$_{10}$. *J. Mol. Biol.* 152:427–443.

Penfold, J., and J. Tomkinson. 1986. The ISIS time-focussed crystal analyser spectrometer, TFXA. Report RAL-86-019. Rutherford Appleton Laboratory, Chilton, UK.

Peto, S., P. Gillis, and V. P. Henri. 1990. Structure and dynamics of water in tendon from NMR relaxation measurements. *Biophys. J.* 57:71–84.

Ramachandran, G. N., and R. Chandrasekharan. 1968. Interchain hydrogen bonds via bound water molecules in the collagen triple helix. *Biopolymers.* 6:1649–1658.

Renugopalakrishnan, V., G. Chandrakasan, S. Moore, T. B. Hutson, C. V. Berney, and R. S. Bhatnagar. 1989. Bound water in collagen: evidence from Fourier transform infrared, and Fourier transform photoacoustic spectroscopic study. *Macromolecules.* 22:4121–3.

Sakakibara, S., Y. Kishida, K. Okuyama, N. Tanaka, T. Ashida, M. Kakudo. 1972. Single crystals of (ProProGly)$_{10}$: a synthetic polypeptide model of collagen. *J. Mol. Biol.* 65:371.

Scott, A. C. 1992. Davydov's soliton. *Phys. Rep.* 217:1–48.

Smith, J. 1991. Protein dynamics: comparison of simulations with inelastic scattering experiments. *Q. Rev. Biophys.* 24:227–291.

Smith, M., A. G. Walton, and J. L. Koenig. 1969. Raman spectra of poly-L-proline in aqueous solution. *Biopolymers.* 8:173–179.

Suck, J.-B., and H. Rudin. 1983. Vibrational dynamics of metallic glasses studied by neutron inelastic scattering. *Top. Appl. Phys.* 53:217–268.

Tageuchi, H., and I. Harada. 1990. Ultraviolet resonance Raman spectroscopy of X-proline bonds—a new marker of hydrogen bonding at the imide C=O site. *J. Raman Spectrosc.* 21:509–515.

Van Zandt, L. L., and V. K. Saxena. 1994. Vibrational local modes of DNA polymer. *J. Biomol. Struct. Dyn.* 11:1149–1150.

Warner, M., S. W. Lovesey, and J. Smith. 1983. The theory of neutron scattering from mixed harmonic solids. *Z. Phys. B Condensed Matter.* 51:109–126.

Wess, T. J., A. Miller, and J. P. Bradshaw. 1990. Cross-linkage sites in type I collagen studied by neutron diffraction. *J. Mol. Biol.* 213:1–5.

White, J. W. 1976. Inelastic neutron scattering from synthetic and biological polymers. *In* Neutron Scattering for the Analysis of Biological Structures. *Brookhaven Symp. Biol.* 27:VI3–26.

Windsor, C. G. 1981. Pulsed Neutron Scattering. Taylor & Francis, London, UK. 432 pp.

Yonath, A., and W. Traub. 1969. Polymers of tripeptides as collagen models IV. Structure analysis of poly(L-prolyl-glycyl-L-proline). *J. Mol. Biol.* 43:461–477.